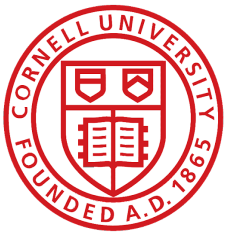

Automated Parametric Workflow for Turbulent CFD Modeling of an Electric Car

Sean Hughes

MAE 4291 Supervised Senior Design Experience
Sibley School of Mechanical and Aerospace Engineering
Cornell University, Ithaca, NY USA

May 23, 2023

Table of Contents

Executive Summary

1. *What are the desired function(s) of your design?*

   The modified car body is meant to reduce drag as much as possible while still balancing consumer needs and preferences. In particular, form drag is expected to be the primary mode of drag on the car; therefore, the car is designed to minimize the pressure differential from the front face to the back face of the car. This allows the car to be as aerodynamic as possible, reducing the energy costs associated with maintaining a desired velocity, and therefore increasing the range of the electric vehicle for the consumer. Reducing drag therefore makes the electric vehicle a more desirable purchase for consumers who might otherwise purchase a car with a more traditional combustion engine. Importantly, the modifications made to improve aerodynamics must not impede upon the car's aesthetics or passenger functionality.

2. *What constraints related to the main function(s) must your design satisfy?*

   The large battery associated with the electric vehicle places a size constraint on the floor of the car that would otherwise not be present. This requires the height of the car to be greater than 1.35 m. Additional important geometric constraints are that the floor of the car must be 0.15 m from the ground, the car width must be 1.5-2.0 m, and finally, the total car length must be 3-6 m. These size constraints create a bounding box for the potential car body shapes such that only realistic geometries can be made. For example, the car floor cannot be too close to the ground as this will invariably cause damage to the car body when driving on inclines or declines, or encountering any normal amount of road debris. Furthermore, the width of the car must be such that it would fit in a standard car lane in the U.S., while the length is such that it does not carry excess weight or high moment of inertia upon turning. Longer vehicles such as semi-trucks require more wheels to stabilize their turning; thus, any length greater than 6 m was out of scope for this project.

3. *What are the performance objectives of your design? (Give quantitative metrics as much as possible).*

   The car's drag coefficient, calculated from ANSYS Fluent, was chosen as the primary performance metric for the design project. Most modern automobiles achieve a

drag coefficient below 0.35, so this was made as the marker for an adequate design. However, the purpose of this paper was primarily to observe the trends associated with the drag coefficient and the geometry of the back of the car. As such, the focus of the results section was not on changing the car to meet a performance requirement, but rather, on seeing how progressively changing the back angle of the car and the height of the backplate would ultimately affect the drag coefficient. Since the drag coefficient is non-dimensionalized with respect to the frontal area of the car, it also accounts for the effect of different car sizes, making it an ideal quantity to compare to cars already on the market.

While the design of a highly efficient electric vehicle was the main quantitative objective of this paper, the other primary goal was to develop a parameterized workflow that integrates Fusion 360 into ANSYS Fluent such that it can be used as a template for future project work at Cornell University. Parametric studies are at the cutting edge of finite-element modeling, as it has seen a rise in popularity with the advent of virtual prototyping in industry. As such, this paper serves as a first example of how CAD geometry can be parameterized and analyzed in ANSYS Fluent to make fast, efficient design decisions. My hope with this senior design project is that my workflow can be used in classes like MAE 4231 to teach students how to parameterize their CFD simulations. The power of this process cannot be understated; over 30 car geometries were tested in this report using turbulent flow modeling, only taking approximately 5 hours to fully complete the simulation. The main time-sink for parameterized studies, such as this, is the initial setup and development of a workflow. Developing these workflows and integrating Fusion 360 into ANSYS Fluent took many weeks of debugging, researching online, and reading relevant software literature. However, with this paper completed and the workflow definitively established, students can be provided with a full step-by-step guide on how to parameterize their CFD study, giving them the opportunity to quickly learn this technique for their own future use in their careers.

4. *What alternative design concepts were considered?*

Two alternative design concepts for the paper were initially proposed. First, much like how the dimples on golf balls result in increased momentum mixing that reduces form drag—and overall drag coefficient as a result—I considered placing dimples over

the car body to investigate if it had a similar effect on the car. The dimples would have likely had an identical microscopic effect, encouraging turbulent flow that mixes the boundary layer's velocity profile. However, the macroscopic effect of delayed flow separation—and therefore lower form drag—was unlikely to occur in the car body. The car body was quite large in size and therefore would have no need for dimples until the flow became quite close to the back of the car where separation occurs. Furthermore, the initial design of the car demonstrated that flow separation was already sufficiently delayed until it reached the end of the car body, where flow separation is essentially impossible to prevent anyways. Therefore, the dimples were not included in the final paper. Second, I considered placing vortex generators along the top of the car to promote turbulent mixing in a similar fashion to the dimples, as this is commonly used in windmill turbines and plane airfoils. However, this was omitted from the paper for the same reason as the dimples: flow separation at highway speeds (60 mph) was already maximally delayed. If the car were to be tested at higher speeds, such as those found in sports cars, then vortex generators or dimples may have had a significant effect. However, given the minimal amount of separation in the expected driving conditions for the electric car, these alternative design concepts were not used. The design concepts considered in this design are limited to solely the geometry of the back of the car. In particular, cars with increasingly large backplates and cars with increasingly high-angled trunks were tested together such that the individual contributions of each dimension on drag could be elucidated. Overall this corresponded to 30 different car geometries investigated through a parametric study in Fluent.

5. *What analyses were used to select among these alternative design concepts?*

The car body was linked from Fusion 360 into ANSYS Workbench such that a parameter object could be made that alters the CAD geometry directly. A "recording block" was made that tracks every change made to the part geometry and CFD setup in ANSYS until the solver is run. The parameter object was then referenced in ANSYS Fluent such that it iterated through the 30 different car geometry conditions, each time repeating the entire sequence of steps and running the solver. This parametric analysis allowed for the entire process of virtual prototyping to be automated.

The CFD simulation that was used for this project was a k-omega RANS turbulent flow model. This model solves for (1) the turbulent kinetic energy (k), (2) the turbulent dissipation rate (ω), and finally (3) the Reynolds-Averaged Navier Stokes equations. The k-omega model assumes that both k and ω follow similar behavior to the average momentum of the fluid, and therefore can be modeled using differential equations that essentially mimic the RANS equation. This model is valid for the flow described in the problem statement, as the flow is at a high enough Reynolds number to be entirely turbulent, therefore negating the need to use a more complex mixed-flow model. The RANS equations are necessary within this flow regime because the losses incurred by turbulent shear forces are of a high enough magnitude that they can no longer be ignored within the momentum conservation equations. Furthermore, the resulting random fluctuations in local flow velocity necessitate the use of the time-averaged velocity such that the differential equations can be solved. The flow was assumed to be statistically stationary such that all of the Reynolds-averaged parameters do not change over time, despite there being local fluctuations still present due to turbulence. This reduces the temporal accuracy of the model, as more significant random fluctuations in fluid flow (e.g., von Kármán vortices) are impossible to resolve accurately using this model. Still, it provides valuable insights into the average flow pattern over the car; given that each simulation is primarily focused on calculating the average drag coefficient of the car over time, it also follows that the RANS equations provide a sufficient level of accuracy of the quantity of interest.

The model assumes that the flow over the car is bilaterally symmetrical; therefore, only half of the car is modeled and simulated. The results of one side were then mirrored onto the opposite side of the car for presentation. Additionally, the law of the wall was used with a y^+ of 50 mm to formulate a boundary mesh that increases the resolution of the fluid flow close to the boundary layer of the car body. In particular, it was used to determine the maximum size of the first mesh element close to the wall. This therefore allowed for a more accurate assessment of turbulent momentum mixing close to the car body, which had a critical effect on delaying flow separation and reducing the drag coefficient of the car. Without this increased local mesh resolution, the simulation would not have provided an accurate prediction of drag trends on the car. Importantly, this mesh

size was not formulated to resolve the viscous sublayer of the boundary directly through direct simulation and instead relies on the law of the wall to extrapolate the flow in this closest layer. This, therefore, caused some errors associated with the drag coefficient calculation for each simulation. Following this setup, the parametric study was run and the drag coefficients were calculated for each iteration; the results were tabulated and input into a response surface optimization in ANSYS. From this, the relationship between the backplate size and the trunk angle—gathered from the parametric study—was then extrapolated to determine the optimal combination of the two that reduces drag for the car body.

Future work could be done to confirm the trends reported in this paper by using a large-eddy simulation (LES) or direct-numerical solver (DNS) approach, such that temporal variability in the flow could be effectively captured. However, this would drastically increase the computational time needed for the simulation. Instead, it would likely be more time-efficient to create downsized physical models and measure their drag coefficients directly from a wind tunnel rather than attempting to formulate a more complex virtual model than the RANS model provided in this paper.

6. *What industry or society standards were used to inform or evaluate your design?*

The design of the car was based upon current modern designs of cars, featuring aerodynamic tear-drop-like shapes. In particular, the front of the car body was made to replicate the shape of a typical sedan using splines to model the inset window commonly featured in such cars. In addition to this, the “zebra view” in Fusion 360 was used to assess the curvature of the entire CAD model, removing any regions of rapidly changing concavity throughout the car body. This analysis is commonly used in assessing UX-focused designs in industry and is particularly prevalent for design wherein aerodynamic ability is paramount. This ensured that there would be no small pockets of recirculating fluid about the car body, as this is explicitly avoided in modern car designs to reduce drag. Furthermore, the comparative drag coefficient value of 0.35 was based on data on modern car drag coefficients in the present literature. Finally, the design needed to replicate the aesthetic appearance of most modern combustion engine automobiles, despite the constraint on car battery size. This was imperative to the design, as the electric vehicle was simulated such that it could eventually be developed into a

market-viable car; without a good aesthetic appearance, the electric vehicle would not be purchased by consumers and would ultimately have little to no environmental impact. Given these considerations, various alterations to the car's design such as a continuously sloping trunk or tear-drop shape were not considered, as consumers are unlikely to purchase a car that so clearly goes against current aesthetic standards.

7. *Which concepts or skills learned in your coursework were applied to the design?*

The skills that I learned in MAE 4230 were invaluable in completing this project. In particular, I utilized my course notes deriving both the incompressible Navier-Stokes equations, the RANS turbulent flow differential equations, and the effect of turbulent mixing at the boundary layer. This electric car design was simulated under turbulent flow conditions using a k-omega turbulent flow solver in Fluent; as such, it was imperative that I understood the governing equations relevant to the design. Additionally, MAE 4230 gave me valuable practical experience in using ANSYS Fluent, particularly in formatting the results via CFD post. I found it quite helpful to reference my old projects from this course and see how to best format the legend, contour plots, and multivariate data as such.

In addition to the more nuanced, detailed content from MAE 4230, I also leaned on MAE 3230 and MAE 4272 as foundation courses in fluid mechanics. The idea of a golf ball allowing for turbulent mixing, as well as the idea to potentially include vortex generators originally came from examples discussed in lecture in MAE 3230. Furthermore, the course's extensive use of Bernoulli's equation in a variety of applications (airfoils, hydraulic pumps, automobiles, spray bottles, etc.) in both classes gave me the insight to use it in this paper as a form of verification. Calculation of the drag coefficient was a key component of each course's practice problems and we often utilized it as a measure to compare different aerodynamic geometries, particularly for airfoils. My experience in performing these calculations became an easy inspiration to use the same analysis in designing a car body here. Furthermore, the engineering communication lessons incorporated into MAE 4272 gave me fantastic insights into how to best prepare this document for the appropriate audience.

Another class that was quite instructive to my work in that senior design was MAE 4530. This course is a semester-long project in computational modeling using

COMSOL. While the software used for simulation was different from ANSYS Fluent, I found that the course was extremely useful in determining what aspects of numerical simulation are the same between all software and potential applications. For example, the course emphasizes reducing both linearization error through changing residual limits and discretization error via a thorough mesh refinement study. Furthermore, the course built upon the groundwork laid by MAE 4230 in presenting fluid mechanics data and developing informative figures. The course focuses less on deriving governing equations—as MAE 4230 does—and instead attempts to elucidate the "black box" of numerical simulation. In particular, I found it quite useful to reference my notes on the finite difference method and finite volume method when completing preliminary assignments to prepare me for the final electric car body design.

Finally, my work on the Cornell Mars Rover team in MAE 1900 and MAE 4900 was crucial in developing my understanding of virtual prototyping. Over the course of approximately five semesters, I worked on a project that used a parametric study in ANSYS structural to optimize the size and geometry of carbon fiber tubes for our rover's robotic arm. In addition to learning about parametric FEA simulations, I also learned how to create CAD drawings in an elegant, highly constrained way while developing a new camera subsystem on the rover. Without this experience in creating complex CAD models, I would not have been able to successfully prepare my car body model for the parametric design such that the front portion of the car remained constant between parameter iterations.

8. *Evaluate your design, relative to its function(s) and constraints. How well did your design meet each of the performance objectives? How well does your design compare to other, existing solutions to the problem?*

The initial design of an electric vehicle using a backplate size of 0.5 m and a trunk angle of 15° was quite efficient and had a drag coefficient of 0.327, immediately reaching my goal of a drag coefficient below 0.35. Most other vehicles on the market have a drag coefficient below 0.35, so this was a great sign to start. After the initial design, the parameterized study revealed that the optimal combination of parameters to reduce the drag coefficient was a backplate size of 0.45 m and a trunk angle of 15°, as this yields an even lower drag coefficient of 0.320. Finally, while much debugging was required to get

the parametric workflow functioning properly, the final setup was relatively robust and easily implementable for a variety of CFD problems. Much of the debugging effort was focused on ensuring that the Fluent mesher was set up initially to handle all possible part geometries; if a mesh error was encountered with one of the parameter combinations, then the entire simulation would stall. However, with a step-by-step guide, the final workflow would require only some cursory knowledge of Fusion 360 and ANSYS Workbench to implement, thus making it ideal as an educational tool for fluid dynamics courses at Cornell University.

9. *What impact do you see your design, if implemented, having upon public health, safety, and human welfare, as well as upon current global, cultural, social, environmental, and economic concerns?*

   Greenhouse gas emissions have been identified as a major contributor to global climate change, with a large fraction of these emissions being due to combustion engine vehicles. By investigating the effects of different geometric parameters on an electric car body, electric vehicles can be made more aerodynamic. As such, electric vehicles can be made to use less energy and therefore increase their available range. The shorter range of electric vehicles is cited as one of the major downsides for consumers choosing between purchasing a conventional combustion engine vehicle and an electric vehicle. Therefore, this analysis allows electric vehicle manufacturers to create more efficient designs with ranges that can effectively compete with more traditional cars.

   Improving upon the design of electric vehicles will help make them more competitive on the market and therefore result in more electric vehicles being used by the population as a whole. Given that electric vehicles are commonly charged via renewable energy sources such as solar or wind power (e.g. Tesla supercharger), this will also help significantly reduce greenhouse gas emissions due to transportation. Increasing the desirability and therefore total usage of renewable energy is necessary to prevent climate catastrophe; designing more efficient electric vehicles is a small, but important step in realizing this goal within the next few decades. The negative effects of continuing usage of combustion engines cannot be overstated. Greenhouse gas emissions deplete the ozone layer, allowing for radiation from the sun to leak into the atmosphere and warm the Earth. The results of this global heating are devastating: increased prevalence of severe storms

and other destructive climate events, rising water levels, higher prevalence of heat-related illnesses and pandemics, and destruction of delicate ecosystems which help regulate the climate. The destructive positive feedback loop of climate change must be intervened with as soon as possible and from all avenues: a more intelligent design of electric vehicles is one such important method to do so.

10. *What format did your design take? For example, is it a complete set of CAD drawings, a working prototype, a full finished product, a system configuration, a process map, or something else?*

    This design was implemented via a parametric CAD model in Fusion 360 that was then imported and subsequently linked with a parametric study in ANSYS Fluent. The finite volume method was therefore used to numerically solve the k-omega RANS equations, with the relevant results plotted and reported here. This form of virtual prototyping was ideal for the design problem, as it essentially nullified the cost associated with building over thirty full-size cars or model cars and then testing them in an expensive wind tunnel. Furthermore, the utilization of a parametric study effectively automated this entire process, saving much time that would have been spent otherwise constructing each individual car model. Given the reduced time and cost of using virtual prototyping in my senior design, I was able to investigate the trends associated with the back plate size and trunk angle with minimal resources. Even still, this analysis provides valuable insights relevant to modern car manufacturers and future projects seeking to build physical models.

11. *Describe each student's role in the design project if it was a group project.*

    This senior design project was independently completed by myself.

1 | Abstract

Electric vehicles are becoming more prominent in the U.S. market as a competitive, environmentally-conscious alternative to more traditional combustion engine vehicles. The use of an electrically-powered vehicle allows for the car to be fueled solely through renewable energy (e.g. wind power, solar power, geothermal), rather than relying on fossil fuels that release greenhouse gasses into the atmosphere and worsen global warming. Given the rising prevalence of electric vehicles and the growing concern of climate catastrophe, this paper was made to examine the effects of different car body geometry parameters on the overall performance of an electric vehicle. In particular, since electric vehicles require a large battery to store energy, instead of having a fuel tank, there are unique geometric constraints that must be overcome to create a high-performance car that consumers will choose to purchase. After modeling these constraints in Fusion 360, the effects of the backplate size and trunk angle on an electric car's coefficient of drag were simulated in ANSYS Fluent using a parametric study of over 30 different cases. I found that as the backplate size increased, the drag coefficient decreased, up until around 0.6 m, when the drag coefficient began to increase thereafter; conversely, as the trunk angle increased the drag coefficient always increased. Following this study, the results were imported into a response surface optimization to determine the best possible parameter values for generic sedan geometry used in this project. I found that the combination of a backplate size of 0.45 m with a trunk angle of 15° was the most optimal, resulting in a low drag coefficient of 0.320. This drag coefficient is around the same values found in most modern combustion-engine cars and is a promising result for the continued development of and usage of electric vehicles. Using virtual prototyping revealed these performance trends without requiring extensive resources, time, or money. This paper therefore also serves as a powerful reminder of the utility of virtual prototyping, specifically for preliminary investigations into complex engineering systems (such as electric vehicles) that would otherwise require expensive testing and empirical research.

2 | Introduction

Greenhouse gas emissions have been identified as a major contributor to global climate change, with a large fraction of these emissions being due to combustion engine vehicles. By investigating the effects of different geometric parameters on an electric car body, electric vehicles can be made more aerodynamic. As such, electric vehicles can be made to use less energy and therefore increase their available range. Range has been considered one of the largest drawbacks to purchasing an electric vehicle, as charging stations may not be interspersed close enough to allow for the car to drive far away from one's home. Thus, car manufacturers have sought to improve on the range of electric vehicles as much as possible. One such way to optimize the range of an electric vehicle is to reduce its drag coefficient as much as possible, as drag is a non-dimensionalized measure of how much force is placed on the car due to the airflow around it. By reducing the drag coefficient of a vehicle, less energy is required to keep the vehicle at a constant velocity, therefore increasing its range as a result. However, electric vehicles also require a large battery that places geometric constraints onto the vehicle which are not present in traditional combustion engine cars. For example, as can be seen in Figure 1, the electric vehicle designed for this paper has a height constraint due to a relatively large battery along the floor of the car. Minimizing the drag coefficient of an electric vehicle, therefore, has unique challenges not encountered in more conventional car manufacturing.

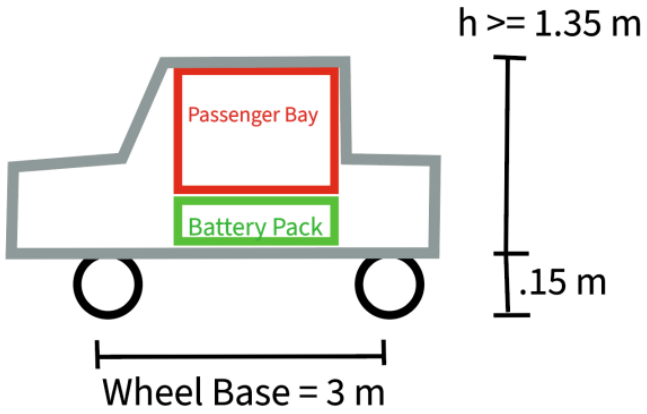

Figure 1. Schematic of the electric car body constraints used for this paper, provided by the MAE 4231 Design Project Statement.

Increasing the range of electric vehicles makes them much more marketable to the general population and increases their competitiveness with combustion engine vehicles. As such, optimizing for the drag coefficient of an electric vehicle may have an indirect effect on reducing carbon emissions by increasing the usage and popularity of electric cars. To that end, this paper seeks to investigate a virtual prototyping workflow that automates the analysis of multiple vehicle trunk geometries such that the most optimal geometry can be found with respect to the drag coefficient. With this knowledge, electric car manufacturers can then utilize virtual prototyping to create an initial design that is much more optimized and requires far fewer iterations of physical prototyping to complete. This, therefore, makes electric vehicle manufacturing more economically viable for manufacturers and establishes a starting point for electric car design that is both convenient and insightful.

3 | Mathematical model

3.1 Modeling Assumptions

The following assumptions were made in formulating the mechanistic model for the electric car:

I. The car is traveling at a constant velocity of 27 m/s (~ 60 mph).
II. The car is traveling at standard sea level conditions: an air density of 1.225 kg/m^3, dynamic viscosity of $1.7894 \cdot 10^{-5}$ kg/m·s, and ambient pressure of 1 atm.
III. The car is bilaterally symmetrical and can be modeled using a simplified two-dimensional shape.
IV. The viscous sublayer of the turbulent boundary layer is not resolved and instead is modeled via the law of the wall for the boundary mesh.
V. The car does not encounter any varying wind speeds, gusts of wind, or rain (i.e. the weather conditions are clear).
VI. The contact region between the wheel and the ground can be modeled as a finite area using a rectangular pedestal.
VII. The car geometry is a rigid body (i.e. does not deform) that retains a constant size and shape over time.
VIII. The surface material properties of the car do not have a significant impact on the flow (e.g. a dirty car vs. a clean car vs. a waxed car) and the car is instead modeled as a smooth surface.
IX. The Reynolds stresses in the airflow can be adequately modeled using the k-omega RANS equations: time-dependent fluctuations in velocity are Reynolds-averaged, the air is an incompressible fluid, and the air is a Newtonian fluid
X. The airflow is *statistically stationary* (i.e. the Reynolds-averaged values of parameters do not change with time).
XI. The effects of gravity on the fluid flow can be ignored.

3.2 Governing Equations

The RANS equations, which include the Reynolds-averaged continuity equation, and the k-omega differential equations are used to model fluid flow. The following unknowns are solved for by the system of equations: $\bar{p}$, $\bar{u}_x$, $\bar{u}_y$, $\bar{u}_z$, k, ω, μ_t .

$$0 = (\mu+\mu_t)\left(\frac{\partial^2\overline{u_x}}{\partial x^2} + \frac{\partial^2\overline{u_x}}{\partial y^2} + \frac{\partial^2\overline{u_x}}{\partial z^2}\right) - \rho\left(\overline{u_x}\frac{\partial\overline{u_x}}{\partial x} + \overline{u_y}\frac{\partial\overline{u_x}}{\partial y} + \overline{u_z}\frac{\partial\overline{u_x}}{\partial z}\right) - \frac{\partial\overline{p}}{\partial x} \quad (1)$$

$$0 = (\mu+\mu_t)\left(\frac{\partial^2\overline{u_y}}{\partial x^2} + \frac{\partial^2\overline{u_y}}{\partial y^2} + \frac{\partial^2\overline{u_y}}{\partial z^2}\right) - \rho\left(\overline{u_x}\frac{\partial\overline{u_y}}{\partial x} + \overline{u_y}\frac{\partial\overline{u_y}}{\partial y} + \overline{u_z}\frac{\partial\overline{u_y}}{\partial z}\right) - \frac{\partial\overline{p}}{\partial y} \quad (2)$$

$$0 = (\mu+\mu_t)\left(\frac{\partial^2\overline{u_z}}{\partial x^2} + \frac{\partial^2\overline{u_z}}{\partial y^2} + \frac{\partial^2\overline{u_z}}{\partial z^2}\right) - \rho\left(\overline{u_x}\frac{\partial\overline{u_z}}{\partial x} + \overline{u_y}\frac{\partial\overline{u_z}}{\partial y} + \overline{u_z}\frac{\partial\overline{u_z}}{\partial z}\right) - \frac{\partial\overline{p}}{\partial z} \quad (3)$$

$$\frac{\partial\overline{u_x}}{\partial x} + \frac{\partial\overline{u_y}}{\partial y} + \frac{\partial\overline{u_z}}{\partial z} = 0 \quad (4)$$

$$\mu_t = \frac{\rho k}{\omega} \quad (5)$$

$$\frac{\partial(\rho u_j k)}{\partial x_j} = \rho P - \beta^*\rho\omega k + \frac{\partial}{\partial x_j}\left[\left(\mu + \sigma_k\frac{\rho k}{\omega}\right)\frac{\partial k}{\partial x_j}\right], \quad \text{with } P = \tau_{ij}\frac{\partial u_i}{\partial x_j} \quad (6)$$

$$\frac{\partial(\rho u_j \omega)}{\partial x_j} = \frac{\alpha\omega}{k}\rho P - \beta\rho\omega^2 + \frac{\partial}{\partial x_j}\left[\left(\mu + \sigma_\omega\frac{\rho k}{\omega}\right)\frac{\partial\omega}{\partial x_j}\right] + \frac{\rho\sigma_d}{\omega}\frac{\partial k}{\partial x_j}\frac{\partial\omega}{\partial x_j} \quad (7)$$

where μ (kg/m·s) is the dynamic viscosity of the air, μ_t (kg/m·s) is the turbulent viscosity, $\bar{u}$ (m/s) is the Reynolds-averaged air velocity (with the subscripts x, y, and z denoting its cartesian components), ρ (kg/m^3) is the density of the air, $\bar{p}$ (Pa) is the Reynolds-averaged air pressure, k (m^2/s^2) is the turbulent kinetic energy, and ω (1/s) is the turbulent dissipation rate. All other variables used within the k-omega differential equations are input using empirical relationships within ANSYS Fluent and are not reported here.

3.3 Boundary and Initial Conditions

The boundary conditions of the model are aimed at effectively simulating the effects of the car driving at highway speeds without needlessly complicating the model. The model was built using an enclosure that forces the car body itself to be negative space, such that a cut-out of the car is made into a large volume mesh. The enclosure is a rectangular box that extends 20 times the length of the car (110 m) in all directions. The only exceptions were as follows: the

enclosure side facing the front of the car uses 10 times the length of the car (55 m)—as the flow is unlikely to change very much prior to physically interacting with the car—the side which faces the plane of symmetry for the car is flush with the plane (0 m), and the side facing the bottom of the car (i.e. the ground) was flush with the wheel pedestals (0 m). The side of the enclosure which faced the front of the car, the top of the car, and the side of the enclosure opposite the symmetry plane were all used as velocity inlet boundary conditions, as can be seen in Figure 2. Specifically, they were set to a velocity of 27 m/s in the x-direction, therefore simulating the car driving forward at a constant velocity of 27 m/s (60 mph). The other cartesian directions (i.e. u_y *and* u_z) had velocity components of zero due to our assumption of negligible wind gusts and clear weather conditions. The turbulent kinetic energy (k) and turbulent dissipation (ω) were specified using a turbulent intensity of 1% and a turbulent viscosity ratio of 2; these corresponded to a k value of 0.10935 m^2/s^2 and an ω value of 3742.979 1/s. Essentially, instead of modeling stationary air and a moving car, which requires much more computational time and memory, the model is a stationary car with moving air around it. Still, the relative velocity between the air and the car is the same in either case, 27 m/s, thereby allowing for this simplification to be made.

A pressure outlet condition of 1 atm was used for the side of the enclosure facing the rear (i.e. trunk) of the car. This ensured that the flow equilibrated to atmospheric pressure, as expected, when far away from the car itself. A symmetry boundary condition (i.e. zero flux boundary condition for all conservation variables) was used for the enclosure surface flush with the plane of symmetry to enforce that the flow is indeed symmetrical about this plane as well as the turbulent kinetic energy and turbulent dissipation. The side of the enclosure flush with the bottom of the wheel pedestals was set as a moving wall boundary condition with a velocity of 27 m/s to simulate the relative velocity between the car and the ground as it drives. Accordingly, the turbulent kinetic energy and turbulent dissipation were specified identically to the other velocity inlet boundary conditions. Without this moving wall condition, the flow would be excessively slowed down by friction incurred from a stationary ground, reducing the accuracy of the model. Finally, the portion of the enclosed coincident with the car body cut-out (i.e. the car body wall) was set to a no-slip boundary condition; similarly, k was set to 0.

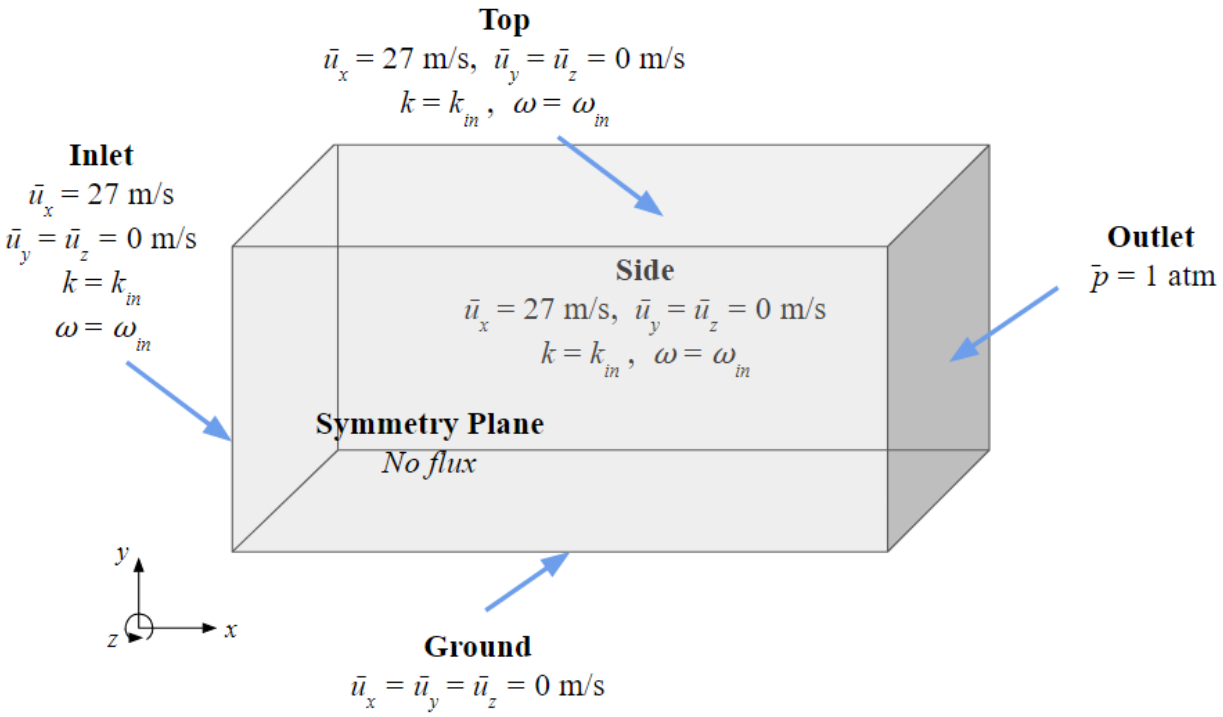

Figure 2. Schematic of boundary conditions implemented for the enclosure in ANSYS Fluent.

4 | Numerical Solution Strategy

4.1 Discretization Error

A mesh refinement study was done on the Ahmed car body prior to the modified car body being created. From this mesh refinement study, it was found that the coefficient of drag for the Ahmed car body converges at around 150,000 elements. In the subsequent investigation of modified car bodies within this report, the same cutoff was used for mesh refinement. All of the simulations included in this report have a total number of mesh volume elements equal to or greater than 150,000 elements, typically reaching values of around 160,000. This mesh, therefore, ensures that the discretization error associated with solving for cell center values of adjacent elements is minimized. As can be seen in Figures 3 and 4, the volume mesh is quite coarse far away from the car body, but quickly reaches a minimum element size of 35 mm closer to the car body surface. Thus, the mesh optimizes computational resources by having a greater cell density closer to the regions with the most fluctuations in fluid velocity.

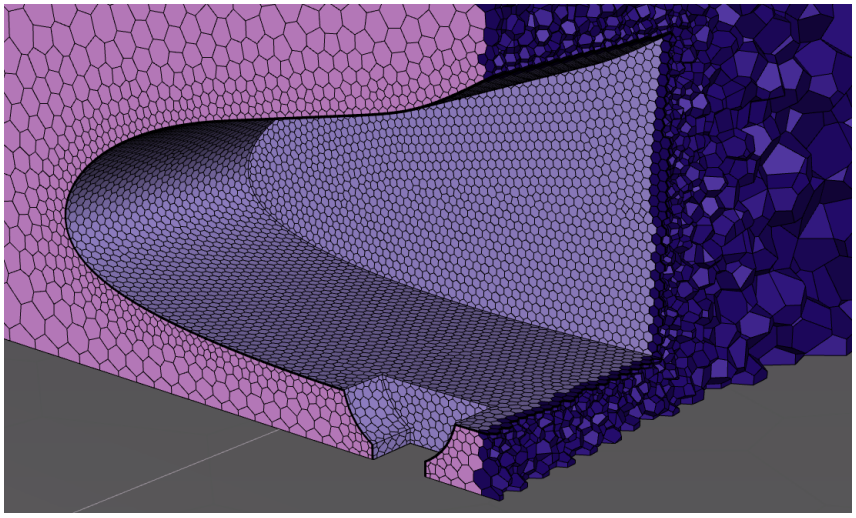

Figure 3. A clipping plane in the z-axis demonstrating the gradual growth of volume elements far from the car wall.

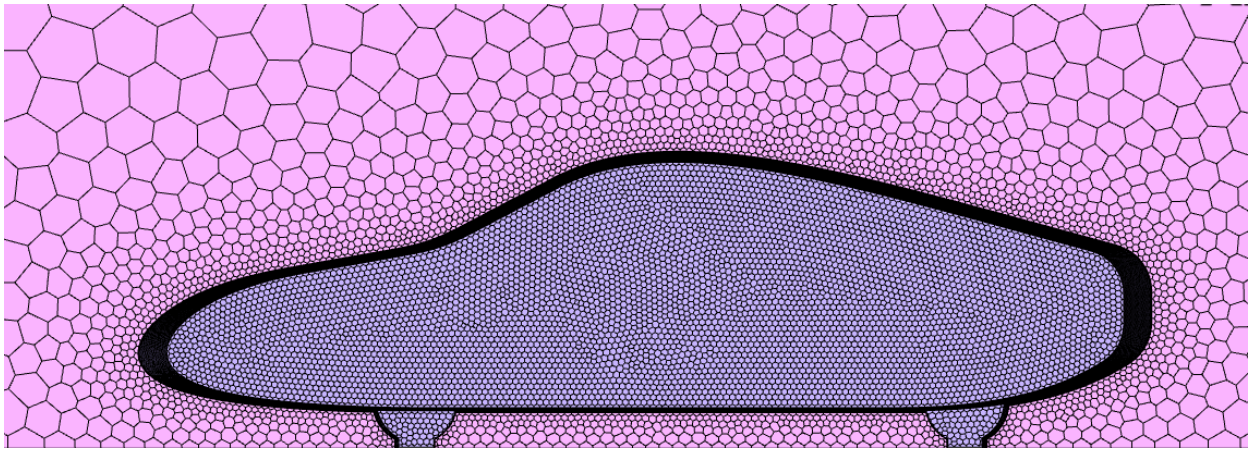

Figure 4. A cross-sectional view of the finite volume mesh used for the car in ANSYS Fluent.

For turbulent flow modeling it was quite important to include an additional boundary layer mesh that increased the resolution of the mesh closest to the car body wall. This allowed for the momentum-mixing effects of turbulent flow at the wall to be calculated via the law of the wall. Without this increased resolution, the buffer layer cannot be resolved and the drag coefficient would have been significantly different. The collective effect of this near-wall momentum mixing ultimately delays the flow separation until it reaches the very end of the trunk of the car. As such, it was imperative that this addition be included to yield accurate results from the simulation. Furthermore, the law of the wall was used with a y^+ of 50 mm to ensure that everything from the buffer layer above could be resolved by the simulation. Importantly, the viscous sublayer was not resolved directly due to y^+ being greater than 1 mm. While in reality, this will cause some additional error to be incorporated into the final results of the study, the effect of the viscous sublayer was still approximated by the law of the wall. The overall trends for drag coefficient could therefore still be elucidated with sufficient accuracy. As such, an initial boundary mesh size of 0.8 mm was calculated, as can be seen in Figure 5. These mesh changes together significantly reduced the effects of discretization error within the final model.

Additionally, a second-order upwind model solver was used in ANSYS Fluent. This solver reduced the discretization error associated with the finite volume method by referencing an additional node upwind from the cell center value when approximating spatial derivatives. This change is necessary to have an accurate solution for turbulent flow regimes due to the large amount of fluctuation that can occur between cell centers.

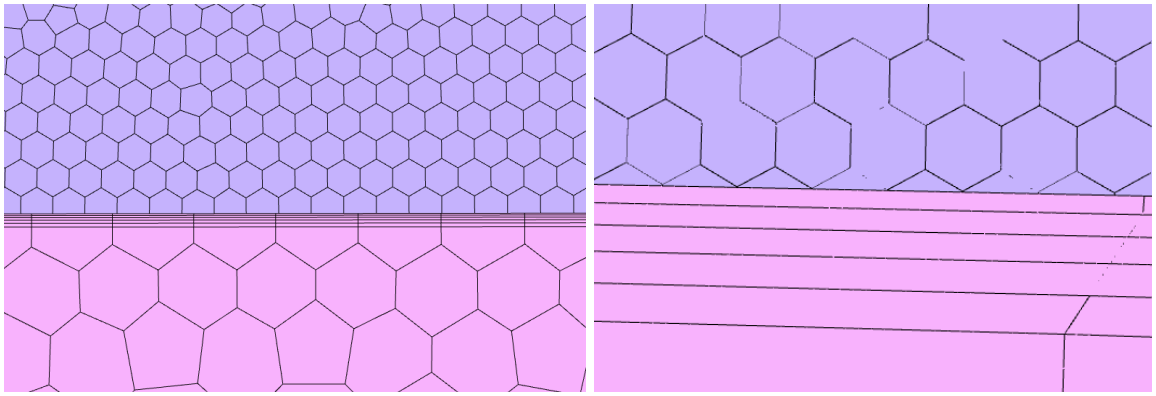

Figure 5. A close-up view of the boundary mesh implemented for the car body demonstrating that the mesh had a much higher resolution close to the car body wall.

4.2 Linearization Error

Linearization error was reduced in this model by using a required residual of 10^{-3} for all conservation equations (RANS, continuity equation, and k-omega differential equations). As can be seen in Figure 6, this ensured that the error associated with linearizing each equation via the finite volume method would be at least lower than a magnitude of 10^{-3}, therefore increasing our confidence in the accuracy of the drag coefficient results. These two modifications to the solver, together, reduced the linearization error a significant amount while still keeping the total computation time relatively reasonable. The average number of iterations required was ~ 80.

The initial guess for the flow parameters was set to be identical to the velocity inlet boundary conditions to simulate the flow only after reaching a statistically stationary state with the car. This meant that the simulation did not model any acceleration of the flow as the car went from 0 to 27 m/s. Instead, the simulation effectively starts when the car has been driving at 27 m/s for quite some time already, such that Reynolds-averaged airflow parameters remain approximately the same with each time step. Importantly, this is not an initial condition for the model because the RANS equations are assumed to be statistically stationary and therefore have no transient terms. Rather, this initial guess is used as the starting value for the iterative solution of the nonlinear algebraic equations.

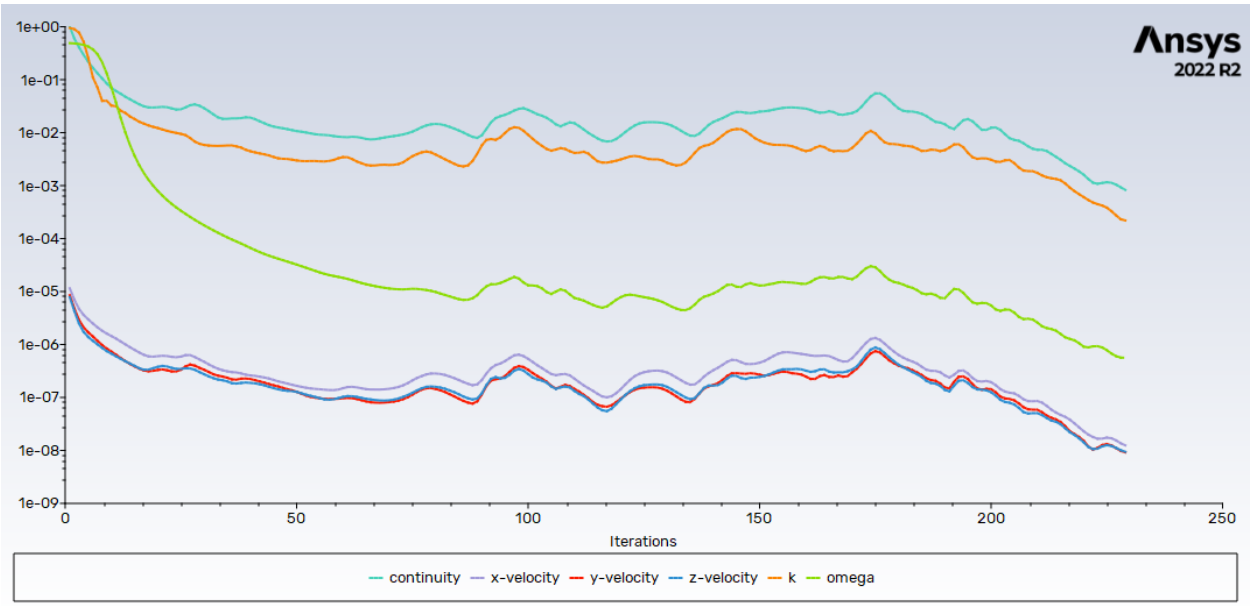

Figure 6. A plot of the residuals decreasing with successive solver iterations in Fluent until all conservation equations (see: *Sec 3.2*) had an associated linearization error less than 10^{-3}.

5 | Initial Design

5.1 Geometry

The geometry of the final design was developed using Fusion 360 CAD. First, bounding boxes were made according to the relevant design constraints using straight construction lines. Following this, splines were fit inside the bounding boxes to create the outer shell of the car. The wheels were then added according to their specified dimensions. The backplate size was parameterized as well as the angle of the spline forming the trunk of the car tangent to the backplate, as can be seen in Figure 7. Following this preliminary sketch being created, the splines were then edited such that the front of the car matched the aesthetic standards of a modern sedan; in particular, the front hood of the car was constrained to have a vertex a short distance above the ground such that the flow would have a clear stagnation point from which to continue either above the car or below. A pedestal was placed at the bottom of each wheel to prevent meshing errors and simulate the bottom of the wheel being flattened by the ground. Only half the car was modeled since the car was assumed to be bilaterally symmetric. Finally, the entire CAD model was extruded and imported to ANSYS as a .stp file. The first design used a backplate size of 0.5 m and a trunk angle of 15°.

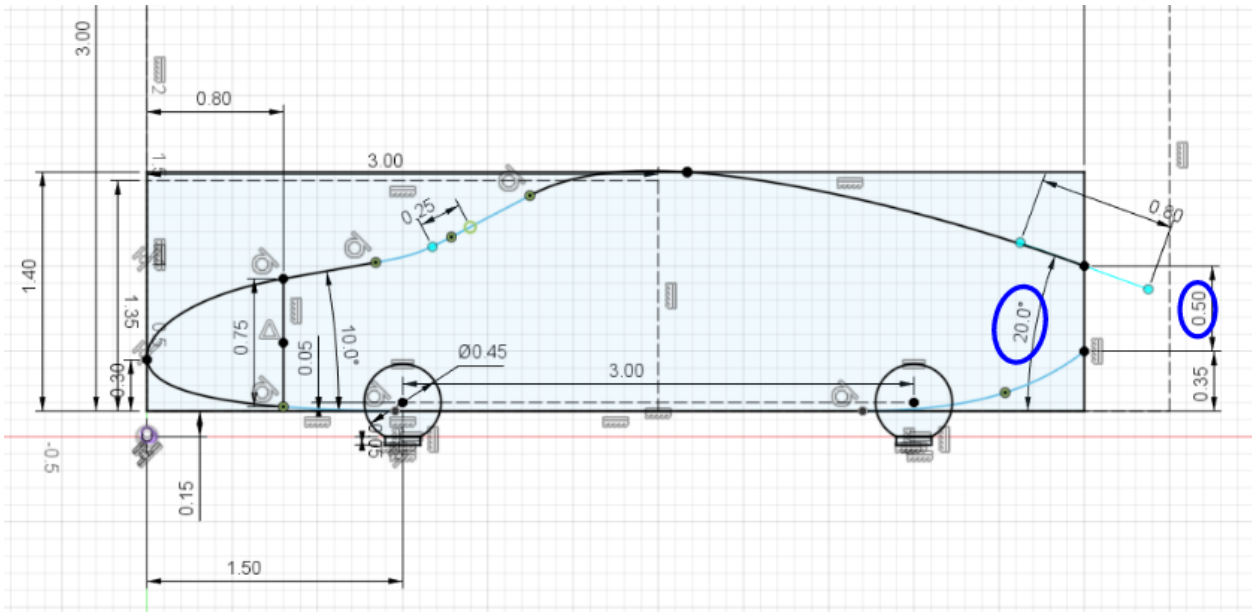

Figure 7. A cross-sectional view of the car body geometry parameterization in Fusion 360; the trunk angle and backplate size are both circled in blue.

5.2 Numerical Results

The solver was changed in the command line to allow for a full multigrid initialization, thereby decreasing the required simulation time without sacrificing accuracy. This first guess value was then used to iterate through solutions until all residuals were below 10^{-3}. As previously stated, the drag coefficient converged to an approximately constant value of 0.327 for the initial design. This value was quite efficient as a starting point for the simulation, as most modern sedans have a drag coefficient that is less than 0.35. Despite this, there are still plenty of more competitive combustion engine cars which boast drag coefficients much lower than 0.327, thus further optimization was needed.

As can be seen in Figure 8 below, the velocity magnitude was highest at the roof of the car and lowest at the vertex of the front hood, as expected. The flow stagnated at this front vertex and then was directed either upwards or downwards, as can be seen in the plot of velocity vectors in Figure 9. If flowing upwards, the air accelerated until reaching a max velocity at the roof of the car, slightly decreasing in velocity as it moved along the trunk until reaching the edge of the car. The velocity magnitude then decreased sharply at the point of flow separation along the back of the car where the trunk ends. This also aligns with our expectations given that the flow should decrease in velocity once entering a recirculation region after separating from the boundary layer. The plot also confirms the efficiency of the initial design by demonstrating that the flow remains attached along the entire trunk of the car, only separating after the car body essentially ends. The recirculation is depicted quite well in the velocity vector plot, which demonstrates how the airflow from the bottom of the car collides with the airflow from the top of the car, causing an exchange of momentum that deteriorates into a turbulent eddy quite quickly. The velocity vectors also confirm the idea that the flow remains attached, as vectors along the back of the car are pointed parallel to the surface of the car at all times. Finally, to further understand the flow around the car body, the pressure contours were plotted in Figure 10. The plot revealed that the highest pressure region was at the vertex of the front hood, while the lowest pressure region was at the top of the car directly after the windshield.

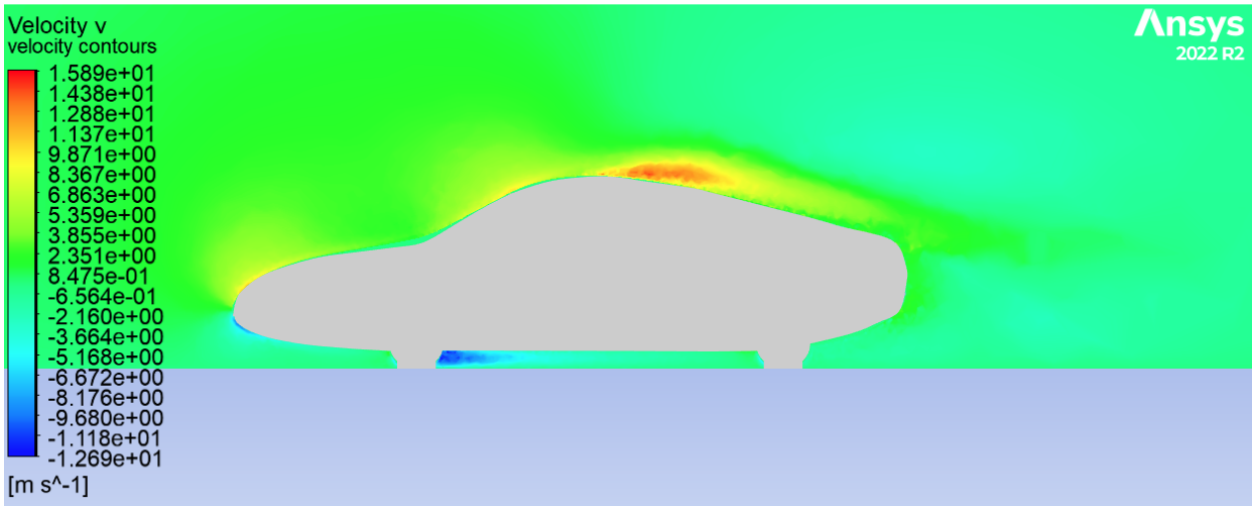

Figure 8. Air velocity magnitude contour plot at the symmetry plane of the car body.

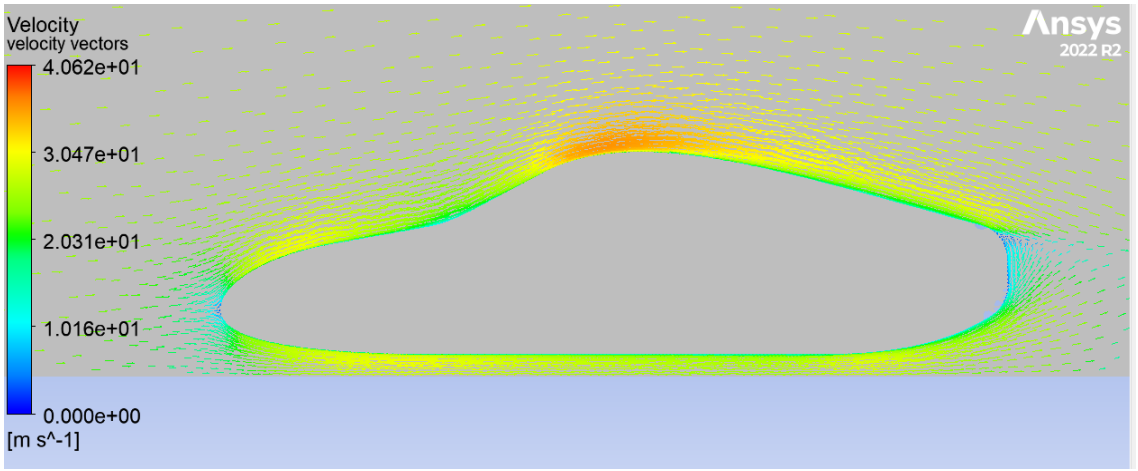

Figure 9. Air velocity vector field at the symmetry plane of the car body.

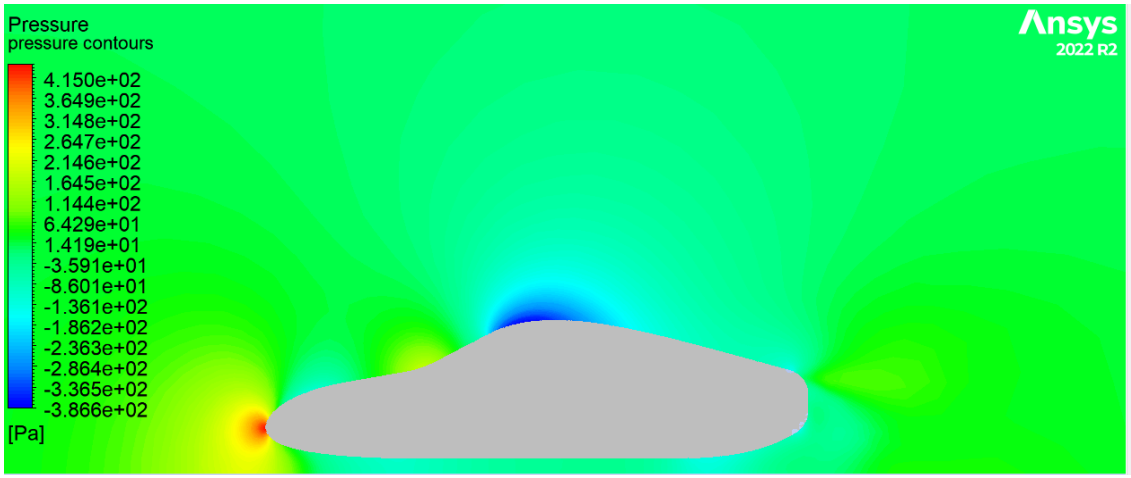

Figure 10. Air pressure contour plot at the symmetry plane of the car body.

5.3 Verification and Validation Steps

The design can be readily verified by employing Bernoulli's principle and looking at the relationship between the pressure contour plot and the velocity magnitude contour plot. Figure 8 shows how the stagnation point is at the front of the car, according to Bernoulli's principle, the dynamic pressure should be zero, therefore the static pressure should increase to its max value. As seen in Figure 9, the pressure contour plot confirms exactly this: the max pressure region was found only at the stagnation point in the front of the car. Using the same logic, Bernoulli's principle correctly predicts that the region of max air velocity at the top of the car should also be the region of the lowest air pressure. The only region in the plot where Bernoulli's principle does not readily apply is the recirculation region behind the trunk of the car, as the total energy of the airflow is decreased by viscous losses and turbulent stress losses; thus, both dynamic and static pressure terms will decrease, causing a decrease in both fluid velocity and pressure simultaneously, exactly as we see in the plots. In addition to verification via Bernoulli's principle, the air velocity magnitude far from the car body is approximately equivalent to the free stream velocity used in our boundary conditions. Similarly, the air pressure far from the car body was approximately equal to 1 atm, which was the pressure boundary condition set for the outlet, as expected. These two analyses, therefore, provide additional confidence that the simulation has indeed solved the mechanistic model accurately as intended.

Despite appearing to solve the model accurately, it is still not clear whether the model does in fact predict the physical behavior of fluid flow around a car; thus, validation of the model itself is also needed. To validate this initial geometry, an empirical study could be conducted using a wind tunnel. A physical miniature model could be 3D printed using the same CAD file used in the simulation, but scaled-down in size, then sanded lightly to smooth the surface. The airspeed could then be set to 27 m/s just as in the simulation, and the drag coefficient could be calculated using strain gauges or a force sensor which measures the pressure difference between the front face of the car and the back face of the car. After multiplying by the frontal area of the car, this gives the form drag across the car, from which the drag coefficient can then be calculated. Skin friction drag will have a much smaller effect on the performance of the car, particularly because each model car will have approximately the same surface material properties; thus, it can be omitted from these comparative empirical calculations.

6 | Design Exploration

After the initial design was established, parameters from the Fusion 360 CAD file were imported into ANSYS workbench directly from Fusion 360 and updated in real-time via a *parameter object* in ANSYS, as seen in Figure 11. A "recording block" was made that tracks every change made during the CFD setup in ANSYS until the solver is actually run. The parameter object was then referenced in ANSYS Fluent such that it iterated through the 30 different car geometry conditions, each time repeating the entire sequence of steps prior to the solver being run. Within the parameter object, a table of values was made such that the backplate size and trunk angle would be iteratively updated to only the desired combinations (see: *Appendix A* for a more detailed walkthrough of the implementation). This parametric analysis allowed for the entire process of virtual prototyping to be automated and the most optimal trunk geometry for the electric vehicle was determined. All of the different vehicle geometries had similar general airflow behavior for air velocity and pressure as discussed previously in *Section 5.2* (i.e. the same trends were found and the same min/max regions were identified for every vehicle). However, the drag coefficient did change significantly between designs. As such, the drag coefficients from each simulation were tabulated in Table 1 for comparison. The backplate size was limited to a max value of 0.6 m, as any value greater than this resulted in the spline forming the back trunk to bend into the front of the car such that it no longer affected solely the back portion of the car. A max trunk angle limit of 35° was also specified to keep the geometry aesthetically realistic; any trunk angle greater than 35° resulted in a vehicle that was significantly deformed compared to most vehicles on the market and had a trunk with essentially no storage capacity.

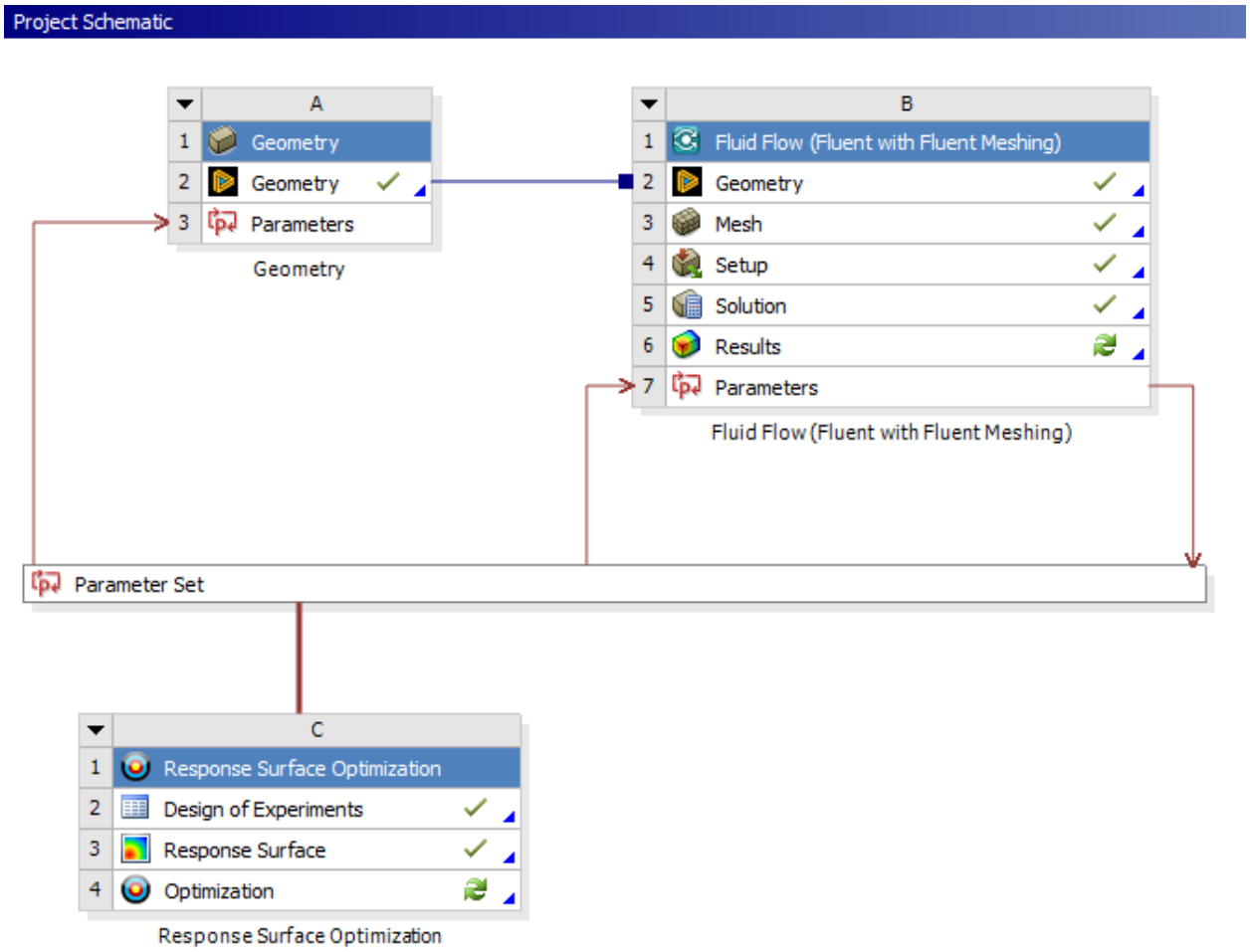

Figure 11. A block diagram depicting the parameter object and response surface implementation in ANSYS Workbench.

Table 1. Drag coefficient values for 30 different potential electric vehicle trunk geometries.

Backplate Height (m)	theta_back (deg)	Simulated Drag Coefficient (C_D)
0.1	15	0.38845
	20	0.39571
	25	0.40511
	30	0.51867
	35	0.68769
0.2	15	0.35011
	20	0.37819
	25	0.38991
	30	0.46312
	35	0.67812
0.3	15	0.33478
	20	0.34329
	25	0.34999
	30	0.35791
	35	0.48713
0.4	15	0.32943
	20	0.33173
	25	0.34523
	30	0.35439
	35	0.45098
0.5	15	0.32715
	20	0.32997
	25	0.33495
	30	0.34621
	35	0.58881
0.6	15	0.32981
	20	0.33411
	25	0.33999
	30	0.34691
	35	0.43123

After solving for all of the parameter design points, the table of drag coefficient values was imported into a response surface optimization object such that the optimal combination of values could be interpolated. The optimization took the 30 combinations already calculated from the parametric study and added 8 additional combinations which interpolate between the lowest drag values reported in the study. The optimization therefore essentially looks at the region of the lowest drag coefficient with a higher resolution to determine an even more optimal combination. The response surface plot varied with respect to two variables—the backplate size and trunk

angle; therefore, the plot was a three-dimensional surface. As shown in Figure 12, the lowest trough in this plot represents the lowest possible drag coefficient out of every possible combination of parameter values. The lowest drag coefficient was found for a backplate size of 0.45 m and a trunk angle of 15°. This makes logical sense, as the lower trunk angle ensures that the flow does not have to sharply accelerate around any corners or turns along the trunk, thus the lowest trunk angle appears to be the most beneficial for delaying separation. The large trunk size follows a similar explanation: the larger the trunk, the smaller the gross angle between the top of the car and the top of the trunk. Therefore, by minimizing both the trunk angle and maximizing the backplate size, to a point, the tangent angle to the edge of the trunk as well as the gross angle between the top of the car and the trunk are both minimized. The parameterized study ran relatively quickly, with each iteration having an average solution time of 10 minutes, thereby making this workflow viable for larger-scale prototyping (e.g. trivariate parameterized studies).

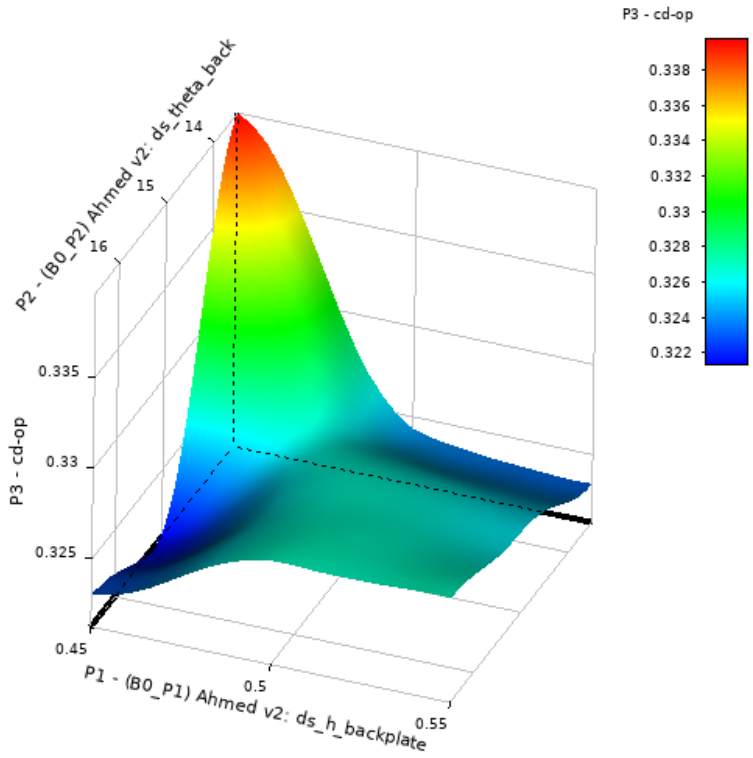

Figure 12. A response surface optimization plot for drag coefficient as it varies with the car's backplate size and trunk angle.

In addition to the response surface optimization, a sensitivity analysis was performed through the parametric study. As can be seen in Figure 13, the analysis found that the backplate size had a more significant effect on the drag coefficient than the trunk angle did. This went against my expectations, as I figured that the trunk angle would more directly affect the airflow separation on the trunk. However, it is an insightful piece of evidence that car manufacturers could use when considering the tradeoffs of different geometric configurations for the car.

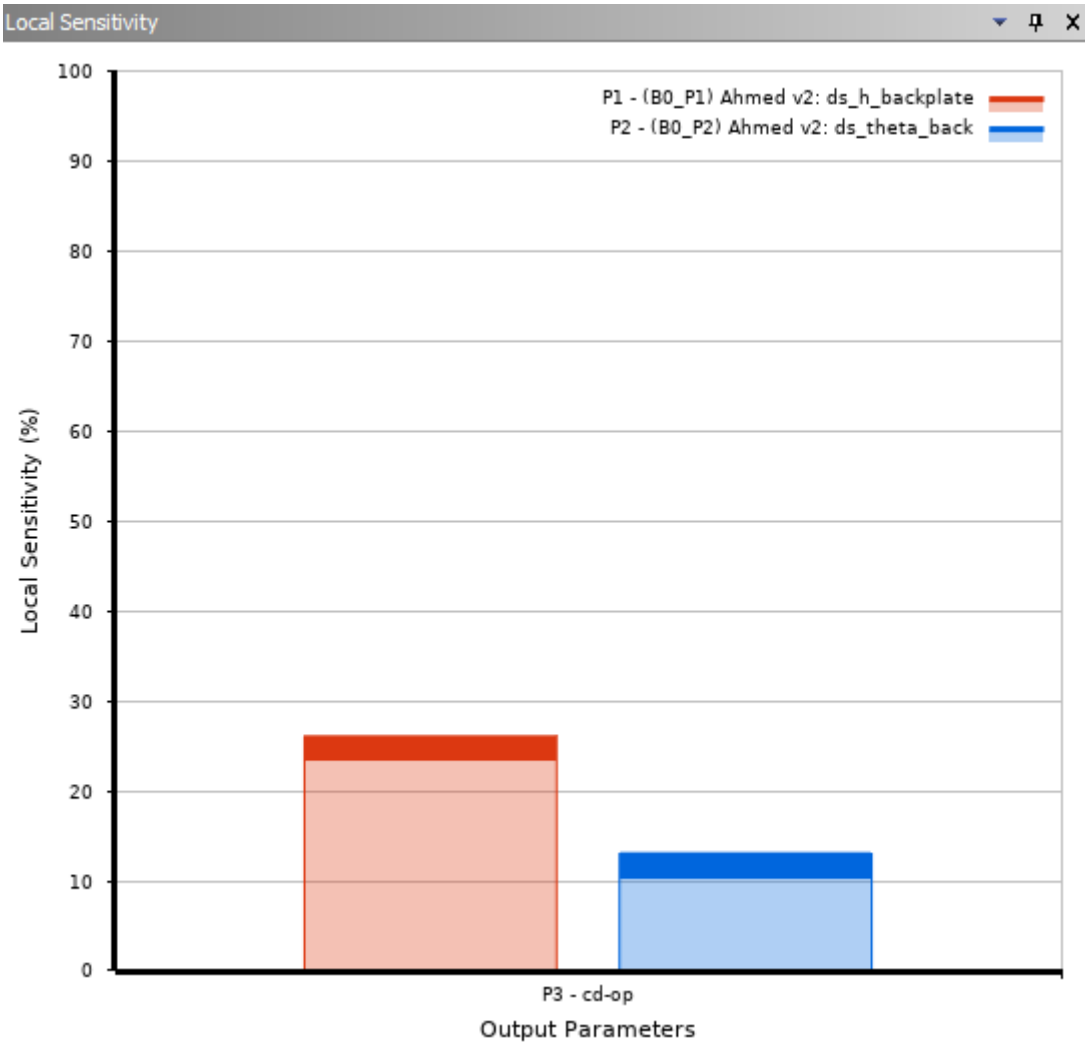

Figure 13. Sensitivity analysis of both geometric parameters demonstrating that backplate size has a greater effect on the drag coefficient compared to the trunk angle.

7 | Conclusions

7.1 Design Recommendations

I found that the combination of a backplate size of 0.45 m with a trunk angle of 15° minimized the drag coefficient of the vehicle as much as possible. A drag coefficient of 0.320 was achieved with these parameter values and was around the same values found in most modern combustion-engine cars. Given these findings, I recommend that electric car manufacturers, particularly for sedans, create their preliminary designs with a trunk angle and backplate size similar to the optimal values found here. In this way, physical prototyping can start at a much more optimal geometry than would have been possible otherwise, thereby saving money, resources, and time for the manufacturer. Additionally, this paper provides valuable insights into the trends associated with changing these parameters; therefore, manufacturers can create more informed decisions when balancing consumer wants and needs. For example, electric vehicle manufacturers can weigh the cost of having a larger trunk size on the performance of the car and decide whether this tradeoff will ultimately be more desirable for customers or not. Altogether, this investigation into virtual prototyping for an electric vehicle empowers car manufacturers to become more efficient in their design process as well as create more informed design choices for their buyers, allowing for electric vehicles to become more competitive on the market and ultimately reduce carbon emissions as a result.

7.2 Limitations

While much effort has been taken to reduce error as much as possible in the mechanistic model used for this report, there are still a few unavoidable errors incorporated into the design. Foremost is that the k-omega Reynolds-averaged Navier-Stokes equations are only valid under an extensive set of assumptions and approximations that, in reality, are scarcely ever true. As such, there is significant error associated with modeling the physical process of turbulent flow. For example, both the turbulent kinetic energy (k) and the turbulent dissipation factor (ω) are assumed to behave according to similar differential equations to the Navier-Stokes equations (i.e. both parameters follow a convection-diffusion process); however, this is purely an assumption and no mathematical derivation exists for the k-omega differential equations. It has simply been

observed that the k-omega equations do tend to predict Reynolds-averaged turbulent flow fairly accurately.

Additionally, to formulate the mechanistic model, the car was assumed to be driving at constant velocity and in essentially perfect weather conditions. It is therefore possible that the chosen geometry is not actually optimal for more adverse weather conditions not accounted for in this model. For example, rain or dirt could alter the surface effects of the boundary layer, wind from other directions (e.g. y or z direction) could alter the observed flow patterns, and a different elevation would alter the airflow parameters like density. Given these assumptions, care must be taken not to extrapolate the results of this simulation to driving conditions that are largely different from the nominal ones investigated here.

Finally, there are clear limitations to the CFD method itself. While the physical modeling of turbulent flow has its own set of limitations, actually solving for the equations introduces additional errors on account of it being a set of multivariable differential equations. Firstly, discretization error is introduced by solving the system of equations only at cell center values and interpolating between them to provide all other values. The conservation equations are intended to be used on a continuum (i.e. a domain with infinite points inside it); however, given the finite computational resources and time available for simulation, this continuum must instead be approximated as a finite set of adjacent control volumes. The farther that cell centers for these control volumes are from one another, the more error that is introduced by interpolation and discretization. In addition to this error, there is also linearization error associated with iteratively solving the equations, starting at a guess value, until there is a sufficiently low residual (i.e. error) between the true value of the equations and the calculated value. Both forms of error were controlled for in this report such that their effects were minimized; however, they will always contribute towards the drag coefficient not being entirely accurate compared to empirically measuring it.

Appendix A

Outline of Schematic B7: Parameters

	A	B	C	D
1	ID	Parameter Name	Value	Unit
2	Input Parameters			
3	Geometry (A1)			
4	P1	(B0_P1) Ahmed v2: ds_h_backplate	0.5	
5	P2	(B0_P2) Ahmed v2: ds_theta_back	15	
*	New input parameter			
7	Output Parameters			
8	Fluid Flow (Fluent with Fluent Meshing) (B1)			
9	P3	cd-op	0.32693	
*	New output parameter			
11	Charts			

Figure A1. Parameter object menu for editing parameter values in ANSYS Workbench.

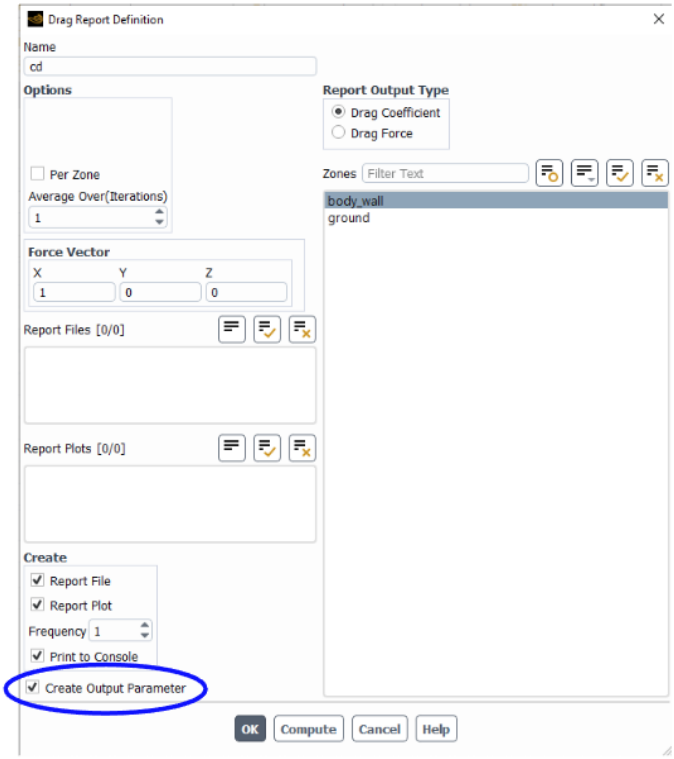

Figure A2. Drag report definition setting used to designate drag coefficient as the output variable for the parametric optimization study.

Table of Design Points

	A	B	C	D	E	F
1	Name	P1 - (B0_P1) Ahmed v2: ds_h_backplate	P2 - (B0_P2) Ahmed v2: ds_theta_back	P3 - cd-op	Retain	Retained Data
2	DP 0 (Current)	0.5	15	0.32693	☑	✓
3	DP 1	0.1	15		☑	
4	DP 2	0.1	20		☑	
5	DP 3	0.1	25		☑	
6	DP 4	0.1	30		☑	
7	DP 5	0.1	35		☑	
8	DP 6	0.2	15		☑	
9	DP 7	0.2	20		☑	
10	DP 8	0.2	25		☑	
11	DP 9	0.2	30		☑	
12	DP 10	0.2	35		☑	
13	DP 11	0.3	15		☑	
14	DP 12	0.3	20		☑	
15	DP 13	0.3	25		☑	
16	DP 14	0.3	30		☑	
17	DP 15	0.3	35		☑	
18	DP 16	0.4	15		☑	
19	DP 17	0.4	20		☑	
20	DP 18	0.4	25		☑	
21	DP 19	0.4	30		☑	
22	DP 20	0.4	35		☑	
23	DP 21	0.5	15	0.32715	☑	
24	DP 22	0.5	20	0.32997	☑	
25	DP 23	0.5	25	0.33495	☑	
26	DP 24	0.5	30	0.34621	☑	
27	DP 25	0.5	35		☑	
28	DP 26	0.6	15		☑	
29	DP 27	0.6	20		☑	
30	DP 28	0.6	25		☑	
31	DP 29	0.6	30		☑	
32	DP 30	0.6	35		☑	

Progress

	A	B	C
1	Status	Details	Progress
2	Updating the Geometry component in Geometry for Design Point 25	Solution Updated	

Figure A3. Table of all possible input parameter combinations iterated through in ANSYS; also shown are the drag coefficients being calculated for 0.5 m backplate geometry combinations.

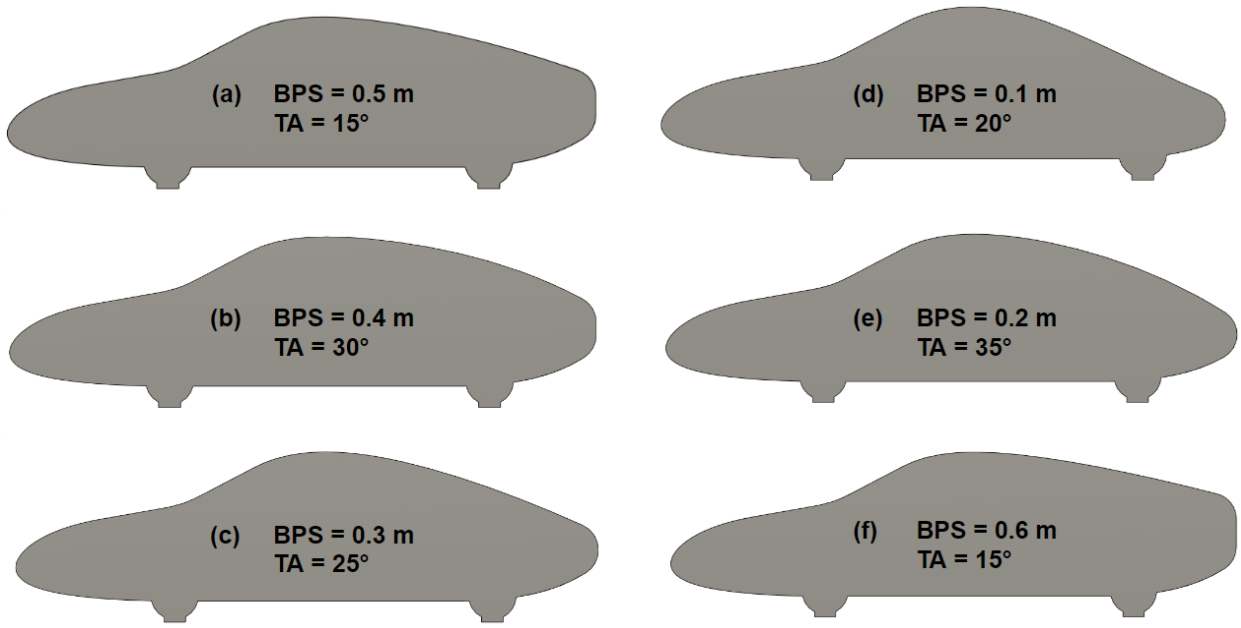

Figure A4. Pictures of multiple different car body parameter combinations imported into ANSYS for simulation; (a) backplate size (BPS) = 0.5 m, trunk angle (TA) = 15°; (b) BPS = 0.4 m, TA = 30°; (c) BPS = 0.3 m, TA = 25°; (d) BPS = 0.1 m, TA = 20°; (e) BPS = 0.2 m, TA = 35°; (f) BPS = 0.6 m, TA = 15°.

Table of Schematic C2: Design of Experiments (Central Composite Design : Auto Defined)

	A	B	C	D
1	Name	P1 - (B0_P1) Ahmed v2: ds_h_backplate	P2 - (B0_P2) Ahmed v2: ds_theta_back	P3 - cd-op
2	1 DP 0	0.5	15	0.32693
3	2	0.45	15	0.32048
4	3 DP 37	0.55	15	0.32573
5	4	0.5	13.5	0.32364
6	5	0.5	16.5	0.32712
7	6 DP 31	0.45	13.5	0.34075
8	7	0.55	13.5	0.32341
9	8	0.45	16.5	0.32314
10	9	0.55	16.5	0.32706

Figure A5. Table of additional geometric parameter combinations solved for by the response surface optimization study in ANSYS Workbench.